Transactions of the 15th International Conference on
Structural Mechanics in Reactor Technology (SMiRT-15)
Seoul, Korea, August 15-20, 1999

Differences in Mechanical Properties and Microstructure of SA 508 CL. 3 Reactor Pressure Vessel Steels Manufactured by Different Steel Refining Process

Se-Hwan Chi[1] and G. E. Lucas[2]

1) Korea Atomic Energy Research Institute, Korea
2) University of California, Santa Barbara, USA

ABSTRACT

Three kinds of SA 508 Cl. 3 reactor pressure vessel steels were examined to evaluate the effect of differences in steel refining practice on the microstructure and mechanical properties. The three refining processes were vacuum carbon deoxidation(VCD), vacuum carbon deoxidation plus aluminum killed (VCDA), and silicon killing and aluminum treated (SA). Results of microstructural examinations and mechanical tests show that the advanced steel making practice of silicon killing and aluminum treated steels (SA) revealed better carbide and bainite lath microstructures. In the case of steels manufactured by VCD, thick interlath carbide layers and incomplete, unclear bainite lath boundaries (BLB) were apparent compared to SA and VCDA steels, suggesting that the material may have experienced uncontrolled heat treatment during the manufacturing process of the thick shell forging material. Despite the microstructural differences the mechanical properties were only slightly different.

1. INTRODUCTION

The embrittlement of pressure vessel steels by neutron irradiation is an important technological problem for the light water reactor industry, as it can dictate the lifetime of the reactor [1]. From the view point of the manufacturer of reactor pressure vessel(RPV) steels, producing RPV steels resistant to embrittlement is an important task. Of those variables relevant to manufacturing process that affect the microstructure of RPV steels, adopted steel refining process are regarded as one of key variables that determine the initial properties and the sensitivity of steels to neutron environments [2].

It is the purpose of the present study to provide a baseline evaluation of the differences in microstructure and mechanical properties of SA 508 Cl. 3 reactor pressure vessel steels manufactured by different steel refining process.

2. EXPERIMENTAL PROCEDURES

2.1. Materials and specimen preparation.

Coupons used for specimen preparation were extracted from four shell forgings which differed in the steel refining process. **Table 1** shows chemical compositions and steel refining process (SRP) of the materials. The heat treatment history of the shell forgings are summarized in **Table 2**. Schematics of each shell forging manufacturing processes are quite similar each other except the major steel refining processes. Coupons, and specimens were machined and prepared from 1/4 T(thickness) locations of the shell forgings. **Figure 1** shows the configuration of specimens for tensile and fracture toughness tests.

2.2 Microstructural examination

The grain size was determined by the three-circle(or Abrams) procedure of ASTM E-112-88, " Standard Test Methods for Determining Average Grain Size" at x 400. Optical microstructures were also examined at x 400.

Investigation of microstructures and carbide morphology was performed by TEM(JEOL 2000FX). To quantify possible differences in a detailed carbide size and density upon materials on TEM, carbon extraction replicas were prepared and examined for precipitates morphologies, and were photographed for precipitates size and density determination.

2.3 Mechanical test

Microhardness tests were performed on hardness disc specimens machined from each coupons where at least 10 indentations per specimens were made for an Hv index at room temperature. Load and duration were 300 g and 20 sec, respectively.

Tensile tests were performed on an Instron 1122, 1,000 pound capacity, screw-driven load frame. Tests were conducted at ambient temperature at a constant displacement rate of 8.5 x 10^{-3}mm/sec. Load-displacement data were recorded on an X-Y recorder and , in addition, the data were digitized and recorded in a computer-based data bank. An average of 500 load-displacement points per specimen were saved.

Fracture tests were performed on MPCC specimens in three point bending over a range of temperatures from the lower shelf to the upper shelf regime : i. e., - 196℃, -150℃, -100℃, -40℃, and 21℃. Althought the specimens were too small to get valid K or J directly at all temperatures ASTM E-399 and E-813 were used as a general guide for testing and data evaluation. Some fracture surfaces of MPCC were examined by JEOL 2111 SEM focusing on the possible differences in fracture morphology especially in the transition region of the materials.

3. RESULTS

3.1 Comparison of microstructures

Comparisons of grain size, precipitate morphology, precipitate number per unit area, and lath microstructure are summarized in **Table 3**. Examples of optical and TEM photos are reproduced in **Fig. 2 and 3.**

All materials show largely the same bainitic microstructure. However, there were some differences in grain size, especially between A and B, C, D. The grain size of A is 50% larger than the B, C and almost double that of D. The absence of aluminum addition in A versus B, C, D can account for the larger grain size.

Round cementites and acicular Mo_2C carbides were found in all steels. No apparent difference was seen in the size of acicular Mo_2C carbides, which were mostly 50 - 100 nm. However, the size of the cementite particle in steel A was about 10 - 20 times larger than that of C and D. Moreover, large agglomerated islands of round cementites were frequently observed in A, but not in D. The size of the agglomerates in A, mostly larger that 30㎛ in length, were larger than the average grain size of A (~22㎛). The number of needle-like Mo_2C was a little higher in A than D. The precipitation of needle-like carbides during tempering is related to the upper-nose temper embrittlement. The long square rod and round carbides in A appear to be precipitated along the lath boundary, but round and needle-like carbides appear to be precipitated along the grain boundary and inside of the lath, respectively.

From the TEM investigations it was found that the lath boundary in A was not developed well compared to B, C, and D. D showed the narrowest lath width(2㎛) and A showed the widest(5㎛). Interlath carbides were found in A, B, and C, and were thickest in A. A low cooling rate during quenching has been attributed to the growth of interlath carbides [3].

3.2 Microhardness, tensile and fracture properties.

Table 4 and **Fig. 4** show microhardness, tensile and fracture toughness test results, respectively. There are no big differences in Vickers microhardness value among the materials. A similarity (B < A, C, D) in yield and ultimate tensile strength(UTS) was observed. There were no significant differences in ductility or work hardening exponent.

Fig. 4 shows the results of the static fracture tests on MPCC specimens of materials A, C, and D. There are relatively few tests, so only general trends can be discerned. Based on these few data, the curve from MPCC appeared somewhat steeper in transition behavior and the transition temperatures indexed at 100 MPa$\sqrt{m}$ were found to be decreased about -67℃ for A and -42℃ for C and D compared to the curves obtained by 1T compact-tension(C-T) fracture toughness specimens [4]. It is seen that there are no big differences between materials in toughness for a test temperature range of -196℃ ~ 21℃. Specimens tested at -196℃ showed linear elastic behavior and elastic-plastic behavior above -150℃. All specimens tested at

-150℃, and A and D specimens tested at -100℃ showed cleavage pop-ins prior to maximun load. As in the case of microhardness and tensile tests, there were not significant differences between materials over the testing temperature range with one exception. A showed a lower effective toughness at -100℃. K_{JC} of A and C were 111.4 MPa$\sqrt{m}$ and 186.4 MPa$\sqrt{m}$, respectively. However, it is well known that scatter in the transition region can be large and hence, the difference in K_{JC} of A and C may result from the statistical nature of cleavage and the inherent scatter in the transition regime than real material differences.

3.3 Comparison of fracture characteristics by SEM fractography

Fig. 5 shows SEM micrograph for A and C tested at -100℃. A shows only a blunting region at the pre-crack tip followed by cleavage fracture, corresponding to the pop-in after small load-line displacement(~10㎛). C shows a region of stable crack growth followed by cleavage, corresponding to the much higher load-line displacement (60㎛) - the ductile tearing probably initiated near max load - and the cleavage pop-in terminating loading.

Figs. 6 and 7 show SEM micrographs of A, C, and D tested at room temperature and - 40℃, respectively. It is seen that cracks grew stably by ductile fracture. As seen in Fig. 8, inclusions observed within the major void were larger in A and C (~10 ㎛) than D (~5 ㎛). As seen in **Fig. 7**, the size and population of inclusion-induced cavities were high in A compared to C and D.

4. DISCUSSION

In spite of many possible differences in the detailed practical steel manufacturing processes, it is expected that no large differences will exist in the microstructure of the steels since all four steels are manufactured to meet the basic requirements of the relevant ASME code. This is the largely the case. However, C and D steels by Si-Al treatment have somewhat better microstructure than A and B. The microstructural differences summarized in **Table 3** can be characterized in terms of (1) grain size, (2) size and distribution of carbides, (3) lath width, and (4) interlath carbides. As stated previously, it seems that steel refining method of Si-Al treatment(C, D) results in better microstructure in grain size, bainite lath structure, carbide size and distribution. Findings of incomplete, unclear BLB with thick interlath carbides in A, for example, demonstrate that uncontrolled heat treatment during the manufacturing process may have contributed to the resultant microstructure in addition to the poor steel refining process of VCD(A).

5. CONCLUSION

From the study of microstructure and mechanical properties of SA508 Cl. 3 RPV steels manufactured by different steel refining process, the following conclusions were drawn.

Interlath carbides and incomplete, unclear lath boundaries were found in steels refined by vacuum carbon deoxidation (A), vacuum carbon deoxidation plus aluminum treatment (B), and a kind of silicon killing and aluminum treatment (C). Especially, steel A of vacuum carbon deoxidation showed comparatively coarse grain size and carbides(cementite) compared to B, C, and D. Lath width, which is regarded as one of the critical metallurgical parameters that determine strength and fracture toughness of bainitic steel, of A was larger than 2.5 times that of D. Distribution of carbides in A was also found agglomerated throughout the matrix bainite comparing to the good dispersion in B, C, and D. In 1/3 sized Charpy fracture toughness testing at transition temperature, A of agglomerated coarse carbides, large grain size, and thick interlath carbides clearly showed cleavage fracture and low fracture toughness in contrast to the ductile crack growth and high fracture toughness in D of well dispersed fine round carbides, small grain size, and free of interlath carbides.

Even few data are available, the results of fracture testing suggest further refining of test and evaluation methods regarding the static test of MPCC for toughness evaluation.

Acknowledgements

This work was carried out under the nuclear R&D program by MOST, Korea. The authors wish to acknowledge for the financial backing provided by MOST which made this work possible. One of the author, Se-Hwan Chi, also wishes to acknowledge Dr. J. H. Hong for his concern on the present work.

Reference

[1] W.L. Server, G. R. Odette, and R. O. Ritchie, " Chapter 3, *Pressurized Water Reactor Pressuree Vessels", in Aging and life Extension of Major Light Water Reactor Component,* Vikram N. Shah, Philip E. Macdonald Eds., Elsevier, 1993, pp. 24 - 93.

[2] Jaroslav Koutsky and Jan Kocik, *Radiation Damage of Structural Materials*, Materials Science Monographs, **79**., Elsevier, 1994, p. 70.

[3] private communication with Y. R. Lim, Seoul Univ., and H. Ohtani, S. Okaguchi, Y. Fujishiro, and Y. Ohmori, *Metallurgical Transactions A* 21A(1990) 877.

[4] J. T. Kim, H. K. Kwon, K. C. Kim, and J. M. Kim, *ASTM STP 1259*, E. G. Nisbett and A. S. Melilli, Eds., ASTM, 1997 (in press) and KAERI/RR-1724/96, J. H. Hong, B. S. Lee, S. H. Chi et al, KAERI (1997).

Table 1. Chemical composition and steel refining process of SA 508 Cl. 3 steel A, B, C, and D which are differ in steel refining process.

Specimen I. D	SRP*	C	Si	Ni	Mn	Cr	Mo	Cu	P	N	Al
A	VCD	0.18	0.08	0.77	1.40	0.15	0.53	0.06	0.005	0.004	<20ppm
B	VCDA	0.17	0.10	0.82	1.35	0.16	0.50	0.03	0.006	55ppm	0.015
C	SA(I)	0.21	0.24	0.92	1.36	0.21	0.49	0.03	0.007	52 "	0.022
D	SA(II)	0.19	0.20	0.82	1.44	0.15	0.55	0.03	0.006	89 "	0.020

SRP*: Steel Refining Process, VCD: Vacuum Carbon Deoxidation,
VCDA: Vacuum Carbon Deoxidation plus Aluminum treatment,
SA(I) and SA(II):Silicon deoxidation plus Aluminum treatment in two different factory, I and II.

Table 2. Heat treatment condition of material A, B, C, and D.

Material	Heat Treatment Condition
A, B, C	Quenching: 650/690℃ (4 hr), 860～900℃ (6 hr) Water quenching to 60℃ Tempering: 650 ～ 670℃ (9～12 hr) Postweld Heat Treatment: 621±14 ℃ (30 hr)
D	Quenching: 870/897℃ (14.2 hr), water quenching Tempering: 650/663℃ (12.4 hr), air cooling Postweld Heat Treatment: 595/625℃ (14.4 hr), furnace cooling

Table 3. Grain size, carbide and precipitates morphology, and bainite lath structure obtained by optical microscope and TEM on thin films and carbon replicas for A, B, C, and D steels.

Material	Grain Size		Precipitates, Carbide, and Bainite Morphology and Lath width(㎛)	Remarks
	ASTM	SIZE(㎛)		
A	7.6	22	Round(dia: ～0.5 ㎛), Fine Needle(50～100nm), Agglomerated, large and localized coarse carbides, Underdeveloped lath boundary, lath width: 5 ㎛ Coarse interlath carbide. PPts No: 6 x 10^7/mm^2 Round:Needle=1:0.85	
B	8.7	15	Round(dia:0.05～0.25 ㎛), Fine Needle(80 nm), Slightly agglomerated, Semi-underdeveloped lath boundary, lath width : 5 ㎛, Interlath carbide, PPts No.: 8.5 x 10^6/mm^2 Round:Needle=1: 22	Incomplete replication
C	8.7	15	Round(dia: 0.025 ㎛, Needle(80nm), Square-like needle(100nm), Three types of carbides morphology, PPts at GB and matrix, Well developed lath boundary, lath width:3.5㎛, Interlath carbides, PPts No.: 3.1x 10^9/mm^2, Round:Needle:Square Needle=1:1.75:0.46.	
D	9.5	12	Round(<0.05㎛), Needle(50～100nm), Fine round carbide, Well developed lath boundary, lath width: 2㎛, No interlath carbides, PPts No.:6.7 x 10^7/cm^2, Round:Needle=1:0.39.	

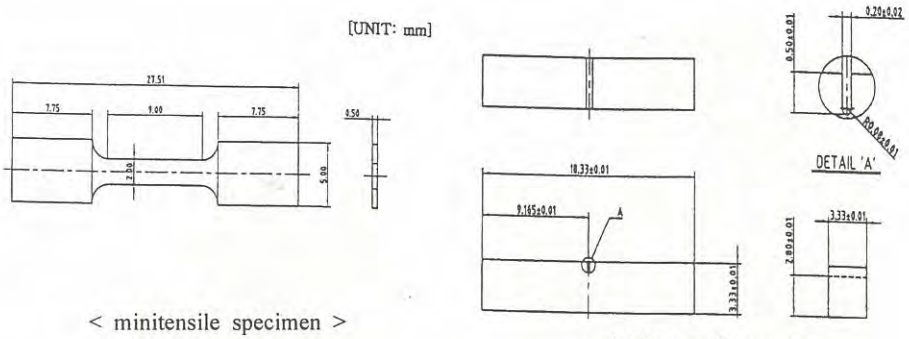

Fig. 1 Configuration of specimens used for tensile and fracture toughness testing.

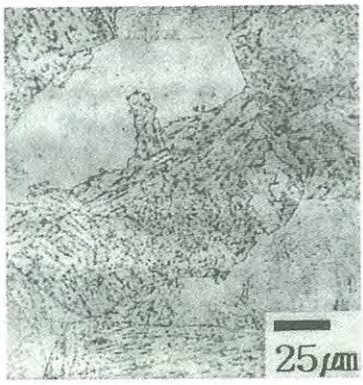

Fig. 2 Optical micrographs of A steel

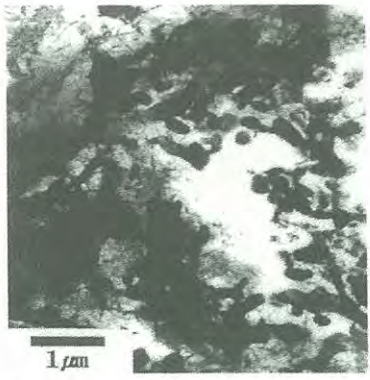

Fig. 3 TEM(thin film) micrographs of the A steel.

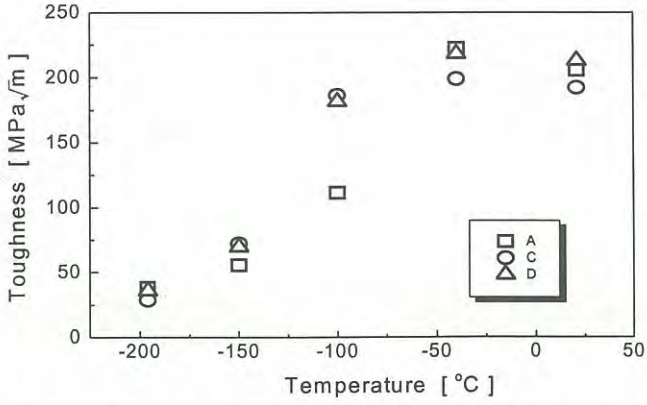

Fig. 4 Static fracture toughness of material A, C and D determined by precracked third size charpy specimen (Testing temp. -196～21℃)

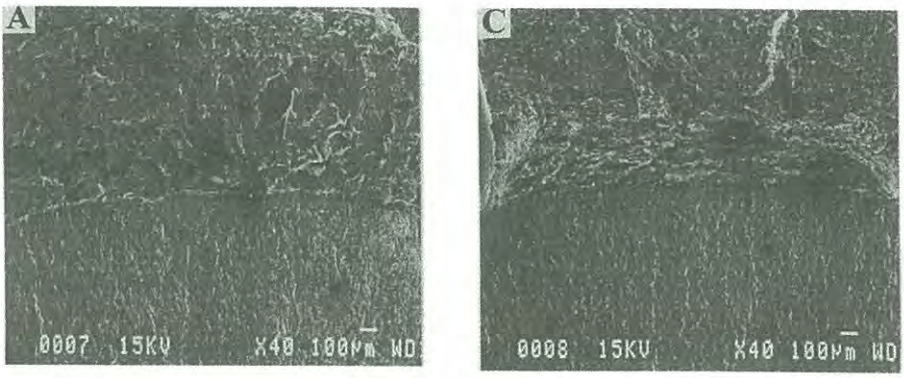

Fig. 5 Comparison of crack extension for MPCC A and C tested at -100℃

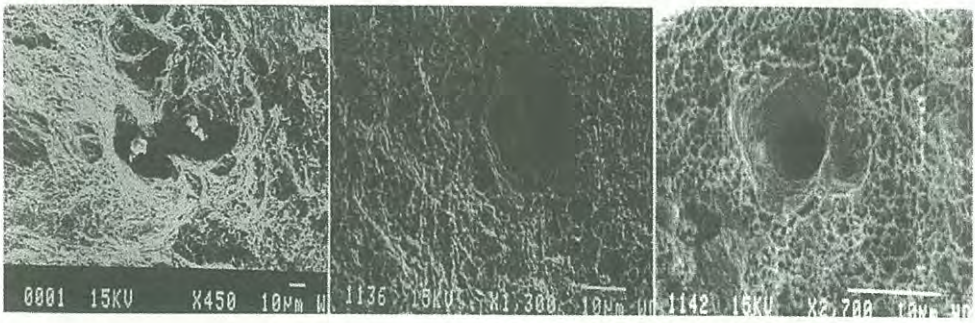

Fig. 6 Inclusions of A, C and D steels. The size of inclusions A and C, i.e ~10㎛, is about double the size of D, ~5㎛. Photos A and C, D were taken from third size Charpy and minitensile specimens, respectively (Test temp. : room temperature).

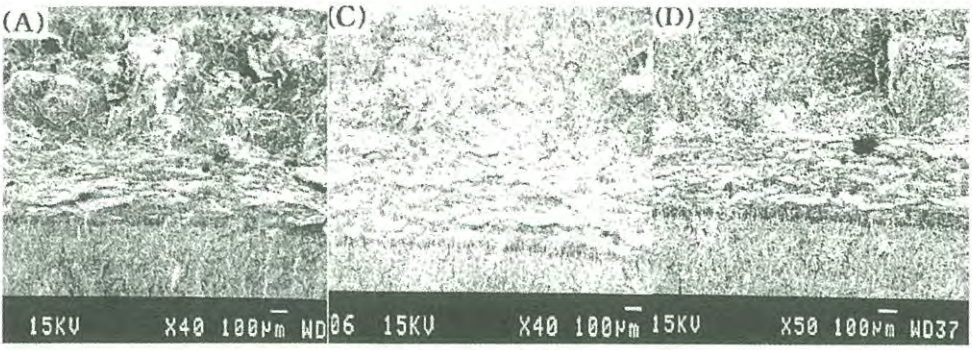

Fig. 7 SEM photos on MPCC tested at -40℃. The size and population of inclusion induced cavities are big and high in A comparing to C and D.